VOLUME 112, NUMBER 12
JUNE 6, 1990

JOURNAL OF THE AMERICAN CHEMICAL SOCIETY

Quantitative Correlations of Heterogeneous Electron-Transfer Kinetics with Surface Properties of Glassy Carbon Electrodes

Ronald J. Rice, Nicholas M. Pontikos, and Richard L. McCreery*

Contribution from the Department of Chemistry, The Ohio State University, Columbus, Ohio 43210. *Received November 27, 1989*

Abstract: Raman spectra, capacitance (C^o), phenanthrenequinone (PQ) adsorption, and heterogeneous electron-transfer rates for ferri/ferrocyanide, dopamine, and ascorbic acid were monitored after fracturing, polishing, and laser activating glassy carbon electrodes (GC-30). Alterations in the Raman spectrum indicate changes in carbon microstructure, while PQ adsorption and C^o provide measures of microscopic surface area. It was observed that polishing caused minor changes in carbon disorder and microscopic surface area, but the polished surface had poor electron-transfer kinetics. Laser activation increased k^o for $Fe(CN)_6^{3-/4-}$ by at least a factor of 200 but increased PQ adsorption and C^o by less than 50% and had negligible effects on the Raman spectrum. A k^o of above 0.5 cm s^{-1} was observed for $Fe(CN)_6$ for the first time. A clean, fractured GC surface exhibited a k^o of 0.5 cm s^{-1} and was very active toward ascorbic acid and dopamine oxidation. The results are consistent with a surface-cleaning mechanism for laser activation, accompanied by little or no observable surface restructuring or roughening. The results on GC are in contrast to those on laser activation of HOPG, where the mechanism involved formation of active sites. The conclusions reached here permit evaluation of the main variables affecting electron-transfer rate for $Fe(CN)_6$, ascorbic acid, and dopamine on GC. We conclude that the active sites for electron transfer are on graphite edges inherent in the GC structure, and the principal function of the laser is exposure of these sites by removal of chemi- and physisorbed impurities.

Carbon has been studied extensively as an electrode material for electrosynthesis, electroanalysis, and electrochemical energy conversion for a variety of reasons.[1-3] The low cost, rich surface chemistry, wide potential range, and compatibility with a variety of electrolytes make carbon an attractive alternative to metals for electrochemistry. Despite wide use, however, there is great uncertainty about the variables that affect the electrochemical behavior of carbon materials, particularly the heterogeneous electron-transfer rate constant (k^o) for redox systems in solution.[4-28] Variations in carbon type and pretreatment history can cause wide variations in k^o for a given redox system, often by many orders of magnitude.[9,29,30] At present there is no consensus about which variables have the greatest effect on heterogeneous electron transfer for carbon electrodes.

One difficulty with addressing the problem is the wide range of materials that share the sp^2 carbon structure, including single-crystal graphite, carbon black, glassy carbon, amorphous carbon, etc. Even when the discussion is limited to one type of carbon, e.g. 2000 °C heat treated glassy carbon (GC-20), surface history causes large variations in k^o. Hu, Karweik, and Kuwana

* Author to whom correspondence should be addressed.

(1) Kinoshita, K. *Carbon: Electrochemical and Physicochemical Properties*; Wiley: New York, 1988.
(2) Sarangapani, S.; Akridge, J. R.; Schumm, B., Eds. *Proceedings of the Workshop on the Electrochemistry of Carbon*; The Electrochemical Society: Pennington, NJ, 1984.
(3) Randin, J.-P. In *Encyclopedia of Electrochemistry of the Elements*; Bard, A. J., Ed.; Dekker: New York, 1976; Vol. 7, pp 1-291.
(4) Stutts, K. J.; Kovach, P. M.; Kuhr, W. G.; Wightman, R. M. *Anal. Chem.* **1983**, *55*, 1632.
(5) Fagan, D. T.; Hu, I. F.; Kuwana, T. *Anal. Chem.* **1985**, *57*, 2759.
(6) Wightman, R. M.; Deakin, M. R.; Kovach, P. M.; Kuhr, W. G.; Stutts, K. J. *J. Electrochem. Soc.* **1984**, *131*, 1578.
(7) Hu, I. F.; Kuwana, T. *Anal. Chem.* **1986**, *58* , 3235.
(8) Deakin, M. R.; Kovach, P. M.; Stutts, K. J.; Wightman, R. M. *Anal. Chem.* **1986**, *58*, 1474.
(9) Hu, I. F.; Karweik, D. H.; Kuwana, T. *J. Electroanal. Chem.* **1985**, *188*, 59.
(10) Kazee, B.; Weisshaar, D. E.; Kuwana, T. *Anal. Chem.* **1985**, *57*, 2739.
(11) Engstrom, R. C.; Strasser, V. A. *Anal. Chem.* **1984**, *56*, 136.
(12) Engstrom, R. C. *Anal. Chem.* **1982**, *54*, 2310.

0002-7863/90/1512-4617$02.50/0

tabulated k° values reported for GC-20 by various labs using different pretreatment procedures.[9] These rate constants varied from $<1 \times 10^{-4}$ to 0.14 cm s^{-1} for $Fe(CN)_6^{3-/4-}$ in 1 M KCl. The highest values reported thus far are in the range of 0.14 to 0.20 and occur after ultraclean polishing, vacuum heat treatment, and laser activation.[21-23]

The many variables that may affect the observed k° for an outer-sphere reaction on GC may be classified into four types. First, the carbon microstructure will affect k°, particularly the fractional density of graphite edge plane on the surface.[29] This variable is most affected by the type of carbon, i.e. graphite, GC, etc. Second, surface roughness will increase the active area available for electron transfer, making k° proportional to the roughness factor provided the scale of the roughness is small relative to $(Dt)^{1/2}$. Third, surface cleanliness has an obvious effect on k° and has been discussed extensively.[6,8,9,11,23,30,31] Finally, the involvement of surface functional groups, particularly oxides, in electron transfer has been invoked to explain several effects of pretreatment, including activation.[15-17,19] Unfortunately, the vast majority of pretreatment procedures, including polishing, oxidation, and heat treatment, affect several or all of these four principal variables. For example, if a particular polishing procedure improves k°, it is not clear whether it does so by increasing roughness, changing edge plane density, forming oxides, or removing impurities. Thus it is difficult to discern which surface variables are important when most procedures alter more than one of the potentially important factors.

In two previous reports, we limited surface variables to only the edge plane density by starting with highly ordered pyrolytic graphite (HOPG) basal plane.[29,32] This surface is initially nearly atomically smooth and clean and exhibits a very low k° for $Fe(CN)_6^{3-/4-}$ until activated with an intense laser pulse. The k° increases by about five orders of magnitude when graphite edges are formed on an initially near-perfect basal plane surface. We concluded that edge plane must be present in order to observe a high k° for $Fe(CN)_6^{3-/4-}$ and dopamine, at least for HOPG, and that the edge plane is the site of electron transfer. Work from several laboratories, including our own, has reported a negative correlation between surface oxides and high k° for $Fe(CN)_6^{3-/4-}$, ascorbic acid, and quinones on GC.[5,6,13,29,30] We concluded that a thick oxide film is not necessary for fast electron transfer to these systems, although the involvement of submonolayer, nonelectroactive oxygen functional groups has not been completely ruled out.[30] Furthermore, the activation of GC is believed to depend on the exposure or creation of active sites that are either absent or covered by impurities on most carbon surfaces.[5,6,23,30] The nature of these active sites is currently unknown.

The current paper discusses changes in GC microstructure, microscopic surface area, and electron-transfer rates upon polishing and activation by pulsed laser irradiation. By monitoring the Raman spectrum, phenanthrenequinone adsorption, and k° for $Fe(CN)_6^{3-/4-}$ during activation, it was possible to identify the principal variable(s) affecting k° and to reveal some characteristics of active sites.

Experimental Section

Raman spectra of GC surfaces were obtained in air as described previously, with 515-nm light and a Spex 1403 spectrometer.[29] Spectral bandpass was 10 cm^{-1}, and typical laser power at the sample was 50 mW. Laser activation was conducted with 1064-nm light as described previously,[21-23,29] with the electrode immersed in solution unless noted otherwise. Laser pulses were applied in groups of three to average spatial and temporal pulse variations. Before measurements of phenanthrenequinone (PQ) adsorption or k° for $Fe(CN)_6^{3-/4-}$, exposure of the GC surface to lab air was avoided by careful exchanges of solutions in the laser activation cell. For example, if the electrode was laser activated in 1 M KCl, a $Fe(CN)_6^{3-}$ solution was introduced by flushing the cell with 1 mM $K_3Fe(CN)_6$ in 1 M KCl, without exposing the electrode to air.

Apparent capacitance was measured as described previously,[32] using a 100-Hz small-amplitude (50 mV) triangular applied potential with $dE/dt = 10$ V s^{-1}. PQ adsorption was determined by the method of Anson,[33] using a solution of 1×10^{-6} M PQ. Cyclic voltammograms were recorded every 5 min until saturation coverage was observed (about 1 h). The area of the PQ reduction peak above the capacitive background was used to calculate Γ_{PQ}. PQ was recrystallized three times from benzene before use. The electrolyte for PQ adsorption was 1.0 M $HClO_4$ for the fractured surfaces. Due to apparent damage to the Torr-seal epoxy during laser activation in $HClO_4$, the PQ adsorption experiments following laser activation were conducted in 1.0 M HCl. Fast scan voltammetry was performed with a triangle wave generator and a digital oscilloscope plus a conventional three-electrode potentiostat and Luggin capillary. Because of the risk of overcompensation, active resistance compensation was not used, and no correction for cell resistance was made when determining k° values.

In order to avoid Fresnel diffraction of the activation laser and to permit fracturing of the glassy carbon in situ, the electrode design used previously[22] was significantly modified. In all experiments except those involving fracturing or fast voltammetry, the electrodes were made from 3 mm diameter GC-30 rod (Tokai). The rod was coated with Torr-seal (Varian) on its side, and the exposed end was polished conventionally with 600 grit SiC paper, 1, 0.3, and 0.05 μm alumina (Buehler). The exposed 3-mm disk was used to measure PQ adsorption, Raman spectra, and slow voltammetry ($\nu \leq 1$ V s^{-1}). The area used to determine Γ_{PQ} (pmol cm^{-2}) was determined from chronoamperometry of $Fe(CN)_6^{4-}$ on a 1-5 s time scale. Background-corrected current vs $t^{-1/2}$ plots were linear in all cases, yielding an area for polished electrodes of 0.075 ± 0.01 cm^2. At high voltammetric scan rates, unacceptable ohmic potential error occurred, and a smaller electrode was required. A GC-30 plate was diamond sawed to produce an approximately 2 cm $\times$ 0.5 mm $\times$ 0.5 mm rectangular solid, which was then coated with Torr-seal. The 0.5 $\times$ 0.5 mm (approximately) face was exposed by polishing, and its area was determined by chronoamperometry of $Fe(CN)_6^{4-}$. The chronoamperometric area varied from electrode to electrode but was typically 0.005 cm^2. The use of Torr-seal raises the possibility of contamination of the surface during polishing. However, the polished surfaces exhibited rate constants comparable to those for polished disks without Torr-seal coatings.

Fractured surfaces were prepared in order to characterize GC surfaces that had not been polished or exposed to lab air. As indicated by Raman spectroscopy, the microstructure of the fractured surface differs from that of the polished surface[34] and should be more representative of the bulk GC structure. However, the fracturing mechanics are strongly dependent on the cross-sectional area of the GC rod being fractured.[35] For the 3 mm diameter rod, the fractured face is heterogeneous, showing a "mirror" region, but also rougher regions visible in a light microscope. The rough regions have very high capacitance (ca. 200 $\mu F/cm^2$) and Γ_{PQ} (ca. 1200 pmol cm^{-2}), perhaps due to microcracking. When the small (0.5 mm $\times$ 0.5 mm) electrodes were fractured, the surface was predominantly mirror-like and had low capacitance (ca. 30 μF cm^{-2}) and Γ_{PQ} (200 pmol

(13) Kovach, P. M.; Deakin, M. R.; Wightman, R. M. *J. Phys. Chem.* **1986**, *90*, 4612.
(14) Wang, J.; Hutchins, L. O. *Anal. Chim. Acta* **1985**, *167*, 325..
(15) Cabaniss, G. E.; Diamantis, A. A.; Murphy, W. R., Jr.; Linton, R. W.; Meyer, T. J. *J. Am. Chem. Soc.* **1985**, *107*, 1845.
(16) Falat, L.; Cheng, H. Y. *J. Electroanal. Chem.* **1983**, *157*, 393.
(17) Gonon, F. G.; Fombarlet, C. M.; Buda, M. J.; Pujol, J. F. *Anal. Chem.* **1981**, *53*, 1386.
(18) Wightman, R. M.; Paik, E. C.; Borman, S.; Dayton, M. A. *Anal. Chem.* **1978**, *50*, 1410.
(19) Kepley, L. J.; Bard, A. J. *Anal. Chem.* **1988**, *60*, 1459.
(20) Hershenhart, E.; McCreery, R. L.; Knight, R. D. *Anal. Chem.* **1984**, *56*, 2256.
(21) Poon, M.; McCreery, R. L. *Anal. Chem.* **1986**, *58*, 2745.
(22) Poon, M.; McCreery, R. L. *Anal. Chem.* **1987**, *59*, 1615.
(23) Poon, M.; McCreery, R. L.; Engstrom, R. *Anal. Chem.* **1988**, *60*, 1725.
(24) Deakin, M. R.; Stutts, K. J.; Wightman, R. M. *J. Electroanal. Chem.* **1985**, *182*, 113.
(25) Evans, J. F.; Kuwana, T. *Anal. Chem.* **1977**, *49*, 1632.
(26) Tse, D. C. S.; Kuwana, T. *Anal. Chem.* **1978**, *50*, 1315.
(27) Moiroux, J.; Elving, P. J. *Anal. Chem.* **1978**, *50*, 1056.
(28) Kamau, G. N.; Willis, W. S.; Rusling, J. F. *Anal. Chem.* **1985**, *57*, 545.
(29) Bowling, R. J.; Packard, R. T.; McCreery, R. L. *J. Am. Chem. Soc.* **1989**, *111*, 1217.
(30) Bowling, R. J.; Packard, R. T.; McCreery, R. L. *Langmuir* **1989**, *58* 683.
(31) Thornton, D. C.; Corby, K. T.; Spendel, V. A.; Jordan, J.; Robbat, A.; Rutstrom, D. J.; Gross, M.; Ritzler, G. *Anal. Chem.* **1985**, *57*, 150.
(32) Rice, Ronald J.; McCreery, R. L. *Anal. Chem.* **1989**, *61*, 1637.
(33) Brown, A. P.; Anson, F. C. *Anal. Chem.* **1977**, *49*, 1589.
(34) Rice, R.; Allred, C.; McCreery, R. L. *J. Electroanal. Chem.* **1989**, *263*, 163.
(35) Dobbs, H. S. *J. Phys. D* **1974**, *7*, 24.

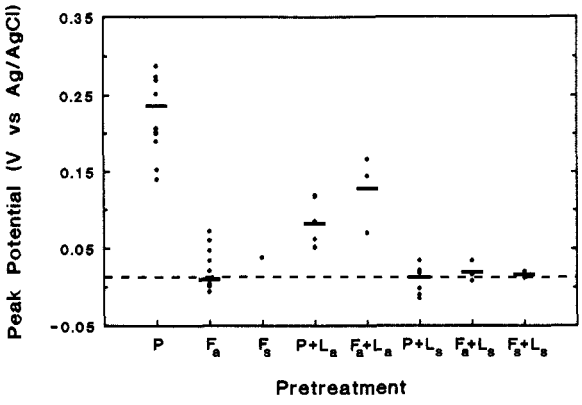

Figure 1. Anodic peak potential (E_p vs Ag/AgCl) for ascorbic acid as a function of GC surface preparation. Points indicate individual experiments; bars are averages. Scan rate = 0.1 V s^{-1}, pH 7.0 buffer. Dashed line indicates reversible E_p observed on Hg electrodes. P, F, and L refer to polished, fractured, and laser activated, respectively, and the "a" and "s" subscripts refer to treatments performed in air or solution.

cm^{-2}). It was essential to use the small electrodes for fracturing experiments in order to produce the mirror surface. Fracturing was accomplished by filing off the Torr-seal from the coated rectangular solid GC, exposing a post about 3 mm long. After the post was scored at the Torr-seal junction, the electrode was placed in the soolution of interest and the post was broken off by impact from the side. The exposed face was used for fast scan voltammetry after positioning the Luggin capillary from the reference electrode <1 mm from the GC face. In all cases (fractured, polished, and laser activated), the area used to determine Γ_{PQ} was the chronoamperometric area determined from a 1–5 s potential step experiment on the electrode in question.

$Fe(CN)_6^{3-/4-}$, dopamine (DA), and ascorbic acid (AA) were used as test systems both because they are sensitive to GC surface preparation and because there is a wealth of comparative data available. Nontrivial uncertainties exist about $Fe(CN)_6^{3-/4-}$ stability and redox chemistry on Pt electrodes,[36,37] but the system appeared well behaved on properly prepared GC surfaces. Unlike its behavior on most carbon electrodes, AA exhibits very fast electron transfer to mercury electrodes. On the basis of voltammetric results on Hg[6,38] the E_p for AA is 20 mV vs Ag/AgCl at pH 7.0. $Ru(NH_3)_6^{2+/3+}$ was examined on laser activated GC-30, but its k° was too large to measure.

Results

Several combinations of laser, polishing, and fracturing pretreatments were compared initially to assess their effects on the ascorbic acid oxidation. This reaction is quite sensitive to surface quality and has been discussed in detail in the literature.[5-7,22] Figure 1 shows the observed peak potential for ascorbate oxidation on GC-20 surfaces treated by polishing, polishing plus laser activation, etc. The horizontal dashed line in Figure 1 is the E_p for AA expected under conditions of rapid electron transfer.[6,38] In addition to the wide range of E_p values observed for GC electrodes, three principal conclusions are evident. First, standard polishing leads to an irreproducible E_p at values significantly positive of $E^{\circ\prime}$, implying a small and variable k°. Second, exposure to air causes increases in E_p values, presumably due to adsorption of airborne impurities. Third, laser activation in solution results in low values of E_p, close to the thermodynamic $E^{\circ\prime}$. If the changes in microstructure, microscopic surface area, and surface cleanliness occurring on the polished surface during laser activation can be determined, both the laser activation mechanism and the factors affecting k° on GC may be revealed. Effects of sample pretreatment on Raman spectra, electrode area, and electrode kinetics will be discussed in turn.

Raman Spectroscopy. As discussed elsewhere, the relative intensities of the 1360- and 1582-cm^{-1} Raman bands provide information about the microstructure of sp^2 carbon, particularly

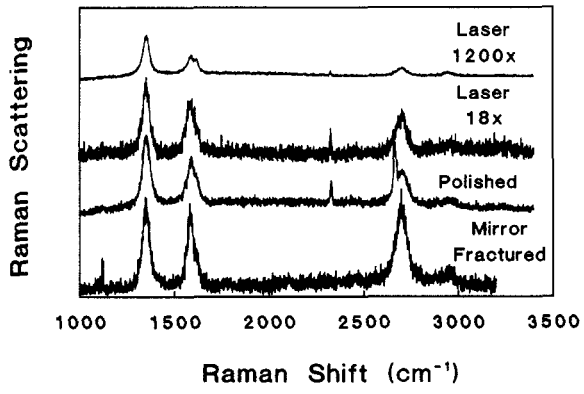

Figure 2. Raman spectra obtained with 515-nm illumination of GC-30 after various pretreatments. Activation laser power density was 25 MW cm^{-2} for the upper two spectra. Laser pretreatments were conducted in water; spectra were obtained in air. The peak at ca. 2300 cm^{-1} is atmospheric N_2; the sharp peak at ca. 2600 cm^{-1} is artifactual.

Table I. Effect of Pretreatments on GC Electrodes

treatment	Raman $I_{1360/1582}$	Raman $I_{2730/1582}$	Γ_{PQ}, pmol cm^{-2}	C°_{obs}, μF cm^{-2}
fractured	1.2	1.00	214 ± 41 (N = 4)[a]	36 ± 5 (N = 6)
polished	1.6	0.80	166 ± 8 (N = 4)	24 ± 2 (N = 5)
laser[b]				
3 × 25 MW cm^{-2}	1.5	0.75	233	29
6 × 25 MW cm^{-2}	1.55	0.60	250	28.5
9 × 25 MW cm^{-2}	1.45	0.80	264	31
12 × 25 MW cm^{-2}	1.4	0.80	252	34
15 × 25 MW cm^{-2}	1.55	0.70	254	35
18 × 25 MW cm^{-2}	1.45	0.75	257	36.5
1218 × 25 MW cm^{-2}	2.1	0.40	ca. 1200	

[a] N indicates number of nearly prepared surfaces. [b] All laser-treated surfaces were initially polished.

the microcrystallite size and edge plane density.[29] A higher ratio of 1360 to 1582 intensity indicates more edge plane and correlates with smaller microcrystallites. Figure 2 shows the effects of polishing and relatively low power density (25 MW cm^{-2}) laser activation on the Raman spectrum of GC-30. The fractured surface was observed initially, since it should most resemble the bulk GC from which all other surfaces are derived. As shown in Table I, the 1360/1582 intensity ratio increases from 1.2 on the fractured surface to 1.6 upon polishing, but it changes little during laser activation. The increase implies exposure or creation of more edge plane (presumably by decreasing microcrystalline size) upon polishing. However, repeated laser activation with up to thirty 25 MW cm^{-2} pulses had little effect on the intensity ratio, implying little change in edge plane density. After more than 1000 laser pulses, the intensity ratio increased above 1.8, indicating significant structural changes. The origin of the band at 2730 cm^{-1} is unclear, but it has been attributed to an overtone of the 1360 band.[39-41] Its intensity is strongly dependent on thermal history[41,42] implying that its intensity is sensitive to carbon microstructure. For GC, the 2730 band intensity decreases upon polishing but remains constant during laser activation, again indicating minor microstructural changes with laser treatment. We conclude that up to thirty 25 MW cm^{-2} laser pulses do not affect the edge plane density or microcrystallite distribution of a polished surface in any way observable by Raman spectroscopy.

Electrode. On the basis of chronoamperometry on a 1–5 s time scale, the macroscopic area of a polished electrode varied slightly with laser activation, with a variation of less than 5% when measured after every third pulse of a sequence of twenty-one 25

(36) Kawiak, J.; Kulesza, P.; Galus, Z. *J. Electroanal. Chem.* **1987**, *226*, 305.
(37) Peter, L. M.; Durr, W.; Bindra, P.; Gerisher, H. *J. Electroanal. Chem.* **1976**, *71*, 31.
(38) Perone, S. P.; Kretlow, W. T. *Anal. Chem.* **1966**, *38*, 1763.
(39) Nemaniah, R. J.; Solin, S. A. *Phys. Rev. B* **1979**, *20*, 392.
(40) Vidano, R. P.; Fischbach, D.; Willis, L. J.; Loeher, T. M. *Solid-State. Comm.* **1981**, *39*, 341.
(41) Lespade, P.; Marchand, A.; Couzi, M.; Crege, F. *Carbon* **1984**, *22*, 375.
(42) Vidano, R.; Fischbach, D. B. *J. Am. Cer. Soc.* **1978**, *61*, 13.

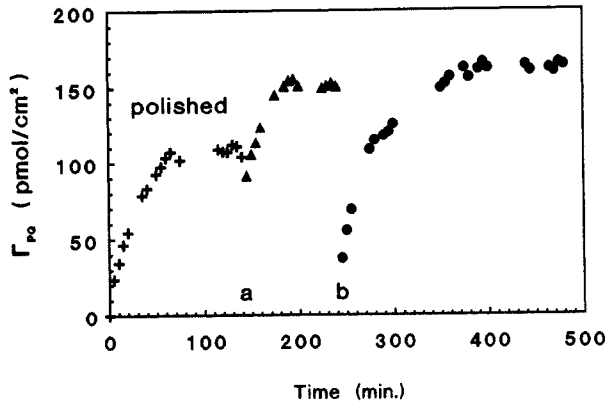

Figure 3. PQ adsorption determined voltammetrically as a function of time and laser treatment. Γ_{PQ} (pmol cm^{-2}) is based on chronoamperometric electrode area. "Polished" refers to the time course of initial PQ adsorption from 10^{-6} M PQ in 1.0 M HCl. At point "a", three 25 MW cm^{-2} laser pulses were applied, and at "b" 18 additional pulses occurred.

MW cm^{-2} laser pulses. The value of 0.075 cm^2 observed throughout laser activation is slightly larger than the geometric area and indicates that no macroscopic changes to the polished electrode are caused by the laser.

The effect of polishing and laser activation on microscopic surface area was assessed by monitoring the adsorption of phenanthrenequinone (PQ) from 1.0 M $HClO_4$ or 1.0 M HCl. For all surfaces, PQ exhibited well-defined voltammograms, which were integrated to determine the amount of PQ absorbed and Γ_{PQ} (mol cm^{-2}), based on the chronoamperometric area. Figure 3 shows the time course of adsorption of Γ_{PQ} during in situ laser activation. After initial adsorption onto the polished surface, three 25 MW cm^{-2} laser pulses cause an increase in Γ_{PQ} of about 42% (Table I). An additional 18 pulses have little effect on Γ_{PQ}. Fractured GC-30 exhibits a PQ surface concentration of 214 ± 41 (N = 4) pmol cm^{-2}, and polishing decreases this value to 166 ± 8 (N = 4) pmol cm^{-2}. Laser activation with three pulses increased Γ_{PQ} over that of the polished surface to a value of 233 pmol cm^{-2}, but further activation increased Γ_{PQ} very slightly. At the power density employed (25 MW cm^{-2}), laser activation produced minor changes (<10%) in Γ_{PQ} after the first 3 pulses, implying minor roughening of the surface by the laser. As an additional but less direct indicator of roughness, the double layer capacity was monitored with the method of Gileadi.[43,44] For the fractured, polished, and laser treated surfaces the square wave current waveform resulting from a triangular applied potential is well defined, although not as well as that for HOPG.[32] The apparent capacitance was independent of triangle wave frequency from 10 to 1000 Hz, indicating minor contributions from Faradaic reactions. As shown in Table I, the observed capacitance increases when the polished surface is laser activated, by about 50% after 18 pulses.

Electrode Kinetics. Table II lists the electrode kinetic data for $Fe(CN)_6^{3-/4-}$, AA, and DA for several pretreatment procedures for GC-30. All kinetic data for $Fe(CN)_6^{3-/4-}$ were obtained with the small (0.5 × 0.5 mm) GC electrode and Luggin capillary in order to minimize ohmic potential error. The fractured surface exhibited significant variation in $k°$ for $Fe(CN)_6^{3-/4-}$, possibly because of small amounts of microcracking caused by the fracturing process.[35] Despite this variation, $k°$ is very high for the fractured surface and is only slightly lower than that for the laser-activated surface.

Peak current vs $\nu^{1/2}$ plots were linear for the fractured (r = 0.9996, ν = 0.1 to 100 V s^{-1}) and polished, laser-activated (r = 0.9999, ν = 100 to 1000 V s^{-1}) surfaces, implying absence of adsorption and adherence to planar diffusion for the scan rates employed. Examples of the variation in $k°$ with scan rate are shown in Table II, and they indicate increasing ohmic error at high (>500 V s^{-1}) scan rates. Attempts to further reduce electrode size to permit higher ν resulted in electrodes with poor performance. The background-corrected voltammogram of $Fe(CN)_6^{3-/4-}$ agrees well with the simulated response for $k°$ = 0.8 cm s^{-1} and ν = 100 V s^{-1}, as shown in Figure 4. The simulated voltammograms for $k°$ values above 0.8 cm s^{-1} were indistinguishable at the 100 V s^{-1} scan rate employed. The results support a $k°$ for $Fe(CN)_6^{3-/4-}$ of 0.5 cm s^{-1} or greater for a laser activated surface, but an accurate value was not obtained because the voltammograms were too close to the reversible limit at the scan rates employed.

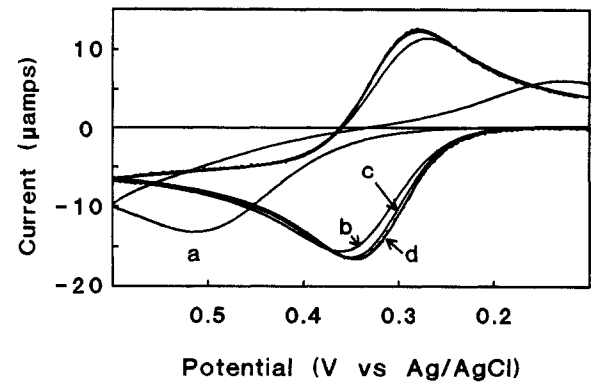

Figure 4. Simulated and observed voltammograms for 1 mM $K_4Fe(CN)_6$ in 1 M KCl on polished, laser-activated GC-30, following eighteen 25 MW cm^{-2} laser pulses. Smooth curves were simulated by using standard explicit finite difference techniques for α = 0.5, ν = 100 V s^{-1}, and $k°$ as follows: (a) 0.005, (b) 0.2 (c) 0.5, (d) 0.8 cm s^{-1}. Noisy curve overlapping curve d is the background subtracted experimental voltammogram. The vertical axis of the experimental curve was adjusted to match curve d.

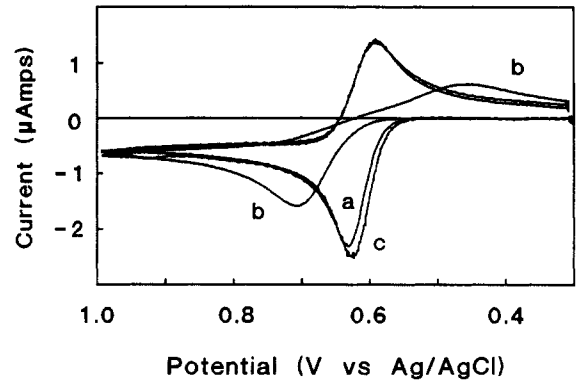

Figure 5. Voltammetry of DA in 0.1 M H_2SO_4, 1 V s^{-1}, all on the same electrode: (a) fractured suface; (b) polished; (c) polished then laser activated with three 25 MW cm^{-1} pulses.

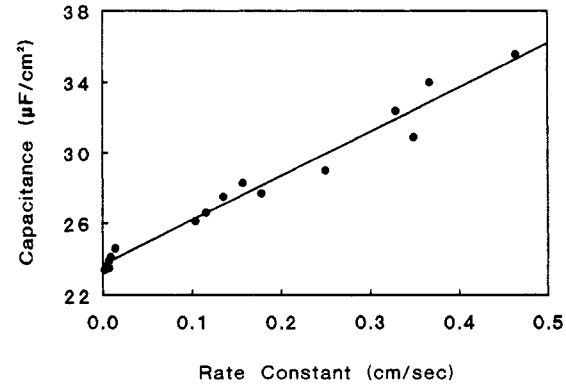

Figure 6. Plots of $C°$ vs $k°$ for a polished, laser-treated surface. Individual $C°$ and $k°$ values were determined on the same surface following each laser pulse. Laser power was increased from 20 to 27.5 MW cm^{-2} in four steps, in order to observe a range of $k°$ and $C°$ values.

(43) Gileadi, E.; Tshernikovski, N. *Electrochim. Acta* **1971**, *16*, 579.
(44) Gileadi, E.; Tshernikovski, N.; Babai, M. *J. Electroanal. Chem.* **1972**, *119* (8), 1018.
(45) Nicholson, R. S. *Anal. Chem.* **1965**, *37*, 1351.

Table II. Electrode Kinetic Parameters for GC-30

treatment	$\Delta E_p(Fe(CN)_6^{3-/4-})$,[a] mV	$k°(Fe(CN)_6^{3-/4-})$, cm s^{-1}	ΔE_p^{DA},[b] mV	E_p^{AA},[c] mV vs Ag/AgCl
fractured	75 ± 6 (N = 8)[d]	0.5 ± 0.2[e] (N = 8)	40	+30
polished	357 ± 49 (N = 7)	0.005 ± 0.003 (N = 7)	252	+220
polished + laser, 3 × 25 MW cm^{-2}	75 ● 4 (N = 3)	0.5 ± 0.1 (N = 3)	34	25
polished + laser, 21 × 25 MW cm^{-2}	<75 (N = 8)	>0.5 (N = 8)		
polished + laser, 3 × 23 MW cm^{-2}				
100 V s^{-1}	91	0.22		
200 V s^{-1}	100	0.23		
500 V s^{-1}	117	0.24		
1000 V s^{-1}	147	0.20		
polished + laser, 12 × 20 and 3 × 23 MW cm^{-2}				
100 V s^{-1}	75	0.46		
200 V s^{-1}	81	0.46		
500 V s^{-1}	96	0.41		
1000 V s^{-1}	117	0.34		

[a] 1 M KCl, 100 V s^{-1} unless noted otherwise, 0.5 × 0.5 mm electrode. [b] 0.1 M H_2SO_4, 0.19 V/s. [c] pH 7.0 phosphate buffer, 0.1 V s^{-1}. [d] N refers to the number of newly prepared surfaces. [e] Determined by the method of Nicholson[45] from ΔE_p.

Figure 5 shows the voltammetric behavior of the dopamine redox system after various pretreatments. Its behavior is qualitatively similar to $Fe(CN)_6^{3-}$, with small ΔE_p on the fractured and laser activated surfaces. Table II includes ΔE_p for DA and E_p for AA oxidation on fractured, polished, and laser-activated GC-30. For both redox systems, the fractured and laser-treated surfaces exhibit much faster kinetics than the polished surface, and ΔE_p and E_p are close to their limits for fast electron transfer. Finally, Figure 6 shows a plot of $k°$ for the $Fe(CN)_6^{3-/4-}$ system vs $C°$, with both parameters determined on the same series of surfaces. The laser power was increased gradually from 20 to 27 MW cm^{-2} so that activation was not completed all at once. It was verified that Γ_{PQ} did not change during the 3rd to 21st laser pulses, even though the laser power was increased.

Discussion

The observation of Raman spectra and Γ_{PQ} during laser activation eliminates two of the major possible mechanisms for $k°$ enhancement. The small changes in 1360/1582 peak intensity ratio indicate that the activation laser does not induce major structural changes, at least in the region sampled by the Raman laser beam. We showed earlier that different carbon types exhibit major differences in both Raman intensity ratio and observed $k°$, with a higher 1360/1582 intensity ratio indicating higher edge plane density and higher $k°$.[29] The relatively high intensity ratio for polished or fractured GC-30 would be expected to support a high $k°$. More to the point, the ratio does not change greatly with laser activation of the polished surface, so the rate enhancement is not accompanied by an increase in edge plane density. We conclude that laser activation must depend on a mechanism other than edge plane creation, at least for GC-30.

An important issue in interpreting Raman spectra is the relative penetration depths of the Raman laser and the pretreatment procedures. The Raman laser samples a depth of about 200 Å, based on the optical constants of GC.[46] Since the Nd:YAG laser has a longer wavelength than the Ar^+ laser used for Raman (1064 vs 515 nm), the activation laser penetrates much deeper into GC. It is therefore reasonable to infer that the region sampled by the Raman laser is thin relative to that affected by the activation laser and that laser activation has minimal effects on Raman observable structural properties of the near-surface layer.

Since polishing affects the Raman spectrum of fractured GC-30, it is clear that polishing effects are deeper than the Raman sampling depth and that polishing has a substantial effect on edge plane density. Since the smallest alumina particle size used for polishing is 500 Å, it is not surprising that polishing effects are hundreds of angstroms deep. XPS analysis of polished GC revealed that polishing introduces oxygen to a depth of 200 Å or more.[28] In addition, laser activation has little effect on the Raman spectrum of the polished surface, implying that the activation laser is affecting a layer that is thin relative to polishing damage. We reported previously that 25 MW cm^{-2} laser pulses removed GC-20 at an average rate of ca. 3 Å per pulse,[23] implying that ablation removes a GC layer that is thin relative to the polished layer. Thus the Raman data indicate that polishing increases the edge plane density in the ca. 200 Å of GC near the surface but that laser activation of the polished surface has little or no further effect on edge plane density.

The changes in Γ_{PQ} during polishing and pretreatment are much smaller than the changes in $k°$, indicating that rate enhancement cannot be a simple consequence of increased surface roughness. For comparison, Brown and Anson report Γ_{PQ} on basal plane pyrolytic graphite of 190 pmol cm^{-2}, close to the fractured value in Table I, and about 14% higher than the polished value. Given the differences in carbon type and surface cleanliness, these differences are probably not significant. On the basis of a molecular area of PQ of 94 $Å^2$ calculated by the method of Soriaga and Hubbard,[47] the observed roughness factor for fractured PQ is 1.21. The decrease to a value of 0.94 upon polishing may be due to decreased surface cleanliness or smoothing of small features on the fractured surface. Laser activation increases the roughness factor to about 1.41, which remains constant with repeated laser pulses. Values near 1.0 may be fortuitous, since blocked adsorption sites may be compensated by roughness or microcracking. In any case, Γ_{PQ} changes by at most 60% upon laser activation of the polished surface, while electron-transfer rates are increasing by factors of more than 100. The observation of minor changes in surface roughness is consistent with other reports that several activation procedures have minor effects on small molecule adsorption on GC.[48]

As shown in Figure 6, $C°$ increases with $k°$ for the laser-activated surfaces, but at a much slower rate. The linear correlation of observed $C°$ with $k°$ shown in Figure 6 was unexpected, but it does permit some useful observations. Since the Raman spectrum and Γ_{PQ} are not changing significantly during the 3rd to 18th laser pulses, the changes in $C°$ and $k°$ must be caused by some other process. A likely candidate is surface coverage by physi- or chemisorbed impurities, which block electron transfer and modify capacitance. As a first approximation, suppose that apparent capacitance is dictated by eq 1, which assumes constant roughness and edge plane density.

$$C°_{obs} = C°_1\theta + C°_2(1 - \theta) \quad (1)$$

where $C°_1$ = capacitance of GC with adsorbed impurities, $C°_2$ = capacitance of clean GC, and θ = surface coverage of chemi- and physisorbed impurities. Furthermore, suppose a similar relation applies to $k°$, as in eq 2.

$$k°_{obs} = k°_1\theta + k°_2(1 - \theta) \quad (2)$$

(46) William, M. W.; Arakawa, E. T. *J. Appl. Phys.* **1972**, *43*, 3460.
(47) Soriaga, M. P.; Hubbard, A. T. *J. Am. Chem. Soc.* **1982**, *104*, 2736.
(48) Bodalbhai, L.; Brajter-Toth, A. *Anal. Chem.* **1988**, *60*, 2557.
(49) Kawiak, J.; Tedral, T.; Galus, Z. *J. Electroanal. Chem.* **1983**, *145*, 163.

After solving eq 2 for θ and substituting in eq 1, eq 3 is obtained.

$$C^\circ_{obs} = \frac{k^\circ_{obs}}{k^\circ_2 - k^\circ_1}(C^\circ_2 - C^\circ_1) + \frac{k^\circ_2}{k^\circ_2 - k^\circ_1}(C^\circ_1 - C^\circ_2) + C^\circ_2 \quad (3)$$

After noting that $k^\circ_2 \gg k^\circ_1$, eq 3 simplifies to

$$C^\circ_{obs} = k^\circ_{obs}\left(\frac{C^\circ_2 - C^\circ_1}{k^\circ_2}\right) + C^\circ_1 \quad (4)$$

Under the assumption of constant roughness and fractional edge plane density (f_e), eq 4 predicts that a plot of C°_{obs} vs k°_{obs} should be linear with an intercept of C°_1, the capacitance of a completely covered surface (Figure 6). A reasonable inference from the linearity of Figure 6 is that both C° and k° depend on surface cleanliness (θ), and therefore each other. Such linearity would not be expected unless roughness and f_e are constant during the series of laser pulses, as demonstrated by Table I. Although a mechanism for laser activation based on surface cleanliness is consistent with all observations presented here, there may be other mechanisms consistent with the experimental results. However, until more is known about the nature of surface impurities, the cleanliness model of eq 1–4 is the most likely possibility.

Referring to Table I, it is clear that the k° observed for polished, laser-activated GC-30 is comparable to that for fractured GC-30. Although there are differences in Raman intensities and Γ_{PQ}, it is clear that the fractured surface is very active toward electron transfer. This observation leads to the important conclusion that exposure of the bulk GC microstructure produces an active surface, without polishing or laser treatment. The fractured surface is at least as active toward DA, AA, and $Fe(CN)_6^{3-/4-}$ as the best surfaces prepared by other methods, including heat treatment, anodization, and ultraclean polishing. The success of an activation procedure for $Fe(CN)_6^{3-/4-}$ or ascorbic acid appears to depend on the extent to which the underlying GC structure is exposed and kept clean. Although the observed k°'s were lower by about an order of magnitude, this conclusion was reached by Jordan et al. after extensive polishing[31] and is related to the discussions of Kuwana et al.[5,9] and Wightman et al.[6,13] regarding surface cleanliness and active sites. Our specific conclusion is that the active sites on GC are on carbon edge planes that are inherent to the GC material. Edge plane density may be increased by polishing, as indicated by Raman spectral changes, but unpolished GC already has a high density of edge plane compared to other forms of carbon such as basal plane graphite. A far more important variable in GC activation is cleanliness. As demonstrated by the large k° for $Fe(CN)_6^{3-/4-}$ on fractured or laser-activated surfaces, the important matter is exposure of inherent sites by the removal of chemi- or physisorbed impurities. As we have stated previously, the conclusion that edge plane carbon contains the active site for electron transfer must be restricted to the systems studied in detail so far, $Fe(CN)_6^{3-/4-}$, AA, and dopamine.

The values of 0.5 cm s^{-1} or higher for k° of $Fe(CN)_6^{3-/4-}$ on fractured or laser-activated GC are of interest when compared to the same redox system on metal electrodes. The highest values in the literature for $Fe(CN)_6^{3-/4-}$ in 1 M KCl are as follows: Au, 0.1 cm s^{-1};[50] Pt, 020–0.26 cm s^{-1};[51] Pt with chemisorbed iodide, >0.1 cm s^{-1};[36] Pt in 1 M KCl, 0.01 M CN^-, >0.1 cm s^{-1}.[36] The relatively narrow variation of k° for fractured or laser-activated GC and three quite different metal surfaces diminishes the likelihood that electron transfer depends on some specific chemical interaction between $Fe(CN)_6^{3-/4-}$ and the electrode surface. Furthermore, the qualitatively similar behavior of AA, DA, and $Fe(CN)_6^{3-/4-}$ on GC argues against any anomaly characteristic of a particular redox system.

The elucidation of the variables that affect k° on GC presented here permits hypothesis of a simple relationship controlling the observed rate constant. Equation 5 assumes that the diffusion layer is much thicker than any surface heterogeneity and that the basal plane or blocked edge plane contribute negligibly to the observed rate.

$$k^\circ_{obs} = k^\circ_{edge} f_e \sigma (1 - \theta) \quad (5)$$

k°_{edge} is the observed rate for clean, smooth edge plane carbon, f_e is the fractional edge plane density, and σ is the roughness factor. For the HOPG basal plane, σ is 1, θ is near zero and f_e is ideally zero (in the absence of defects). Thus k°_{obs} is very small (ca. 10^{-7} cm s^{-1}) because there are no sites, even though the surface is clean. When f_e is increased and sites are created by laser activation of HOPG, k°_{obs} increases greatly, to 10^{-3}–10^{-2} cm s^{-1}.[29,32] For polished GC, f_e is inherently much larger, σ is still near 1, but θ is also near 1. So k°_{obs} is small because of surface blockage by impurities, even though numerous sites are present. Laser activation or fracturing decreases θ, thus increasing k°_{obs}. Thus the laser's main function during activation of HOPG is site creation on a clean surface, while for GC the laser serves to uncover existing sites. As θ is decreased by the laser, both C°_{obs} and k°_{obs} increase (k° much more rapidly), yielding the behavior of Figure 6 and eq 4. At higher power densities, the laser can change f_e and σ, but for the power range employed here, these effects are minor. At least for the systems studied, eq 5 dictates k°_{obs} and incorporates both GC microstructure (in f_e) and surface cleanliness (θ) in the behavior predicted for GC electrodes.

The nature of the surface impurities is unclear, except that they have a pronounced effect on k° and a smaller effect on C°. The simple hypothesis of trace organic adsorbates from the solution or air may be sufficient, but an inhibitory oxide layer should not be ruled out. There is substantial evidence that a thick oxide coating does not enhance k°,[30] and in fact may inhibit electron transfer.[13] Submonolayer oxide films may also decrease k°, and oxide removal may contribute to laser activation. Alternatively, submonolayer oxide coatings may enhance k° for certain redox systems. The effect of controlled oxidation on the kinetics observed on fractured surfaces is currently being investigated.

Acknowledgment. Primary support for the work was provided by the Air Force Office of Scientific Research. Raman techniques and instrumentation was developed under a grant from the National Science Foundation. The authors thank Robert Bowling and R. Mark Wightman for useful discussions, Christie Allred for assistance with obtaining Raman spectra, and Dennis Evans for providing the voltammogram simulation software.

Registry No. GC, 7440-44-0; PQ, 84-11-7; DA, 51-61-6; AA, 50-81-7; $Fe(CN)_6^{3-}$, 13408-62-3; $Fe(CN)_6^{4-}$, 13408-63-4.

(50) Kuta, J.; Yeager, E. *J. Electroanal. Chem.* **1975**, *59*, 110..

(51) Goldstein, E. L.; Van De Mark, M. R. *Electrochim. Acta* **1982**, *27*, 1079.